Journal of Neurochemistry

JOURNAL OF NEUROCHEMISTRY | 2016 | 138 | 624–639 doi: 10.1111/jnc.13697

ORIGINAL ARTICLE

p120-catenin is necessary for neuroprotection induced by CDK5 silencing in models of Alzheimer's disease

Alejandro Uribe-Arias,* Rafael Andrés Posada-Duque,* Christian González-Billault,†,‡ Andrés Villegas,* Francisco Lopera* and Gloria Patricia Cardona-Gómez*

*Neuroscience Group of Antioquia, Faculty of Medicine, University of Antioquia, Medellín, Colombia

†Laboratory of Cell and Neuronal Dynamics, Department of Biology Faculty of Sciences, Universidad de Chile, Ñuñoa, Santiago, Chile

‡Center for Geroscience, Brain Health and Metabolism, Santiago, Chile

Abstract

Cyclin-dependent kinase 5 (CDK5) plays important roles in synaptic function. Its unregulated over-activation has been, however, associated with neurodegeneration in Alzheimer's disease. Our previous studies revealed that CDK5 silencing ameliorates tauopathy and spatial memory impairment in the 3xTgAD mouse model. However, how CDK5 targeting affects synaptic adhesion proteins, such as those involved in the cadherin/catenin system, during learning and memory processes is not completely understood. In this study, we detected reduced expression of p120 catenin (p120 ctn), N-cadherin, and β-catenin in the brain of human Alzheimer's disease patients, in addition to a reduced PSD95 and GluN2B protein levels in a 3xTgAD mouse model. Such decrease in synaptic proteins was recovered by CDK5 silencing in mice leading to a better learning and memory performance. Additionally, CDK5 inhibition or knockout increased p120 ctn levels. Moreover, in a glutamate-induced excitotoxicity model, CDK5 silencing-induced neuroprotection depended on p120 ctn. Together, those findings suggest that p120 ctn plays an important role in the neuronal dysfunction of Alzheimer's disease models and contributes to CDK5 silencing-induced neuroprotection and improvement of memory function.

Keywords: Alzheimer's disease, cadherin/catenin system, CDK5, cognitive function, p120 ctn.

J. Neurochem. (2016) **138**, 624–639.

Cyclin-dependent kinase 5 (CDK5) plays important roles in neuronal functions such as synaptic plasticity, dendritic spine remodeling, neuronal migration, and cognitive processes, including learning and memory (Ohshima *et al.* 1996; Angelo *et al.* 2006; Lalioti *et al.* 2010; Mishiba *et al.* 2014; Mita *et al.* 2014). Under physiological conditions, CDK5 activation requires its interaction with the co-activator p35 or p39 (Ko *et al.* 2001). CDK5 phopshorylates several substrates involved in synaptic activity, which includes the scaffold protein post-synaptic protein 95 (PSD95), the subunit 2B of the *N*-methyl-D-aspartate receptor (NMDA) GluN2B, and adhesion proteins that form the cadherin/catenin system. These proteins are important to support physiological neuronal function, and the aberrant modulations of these proteins have been implicated in neurodegenerative disorders (Kwon *et al.* 2000; Morabito *et al.* 2004; Hawasli *et al.* 2007; Zhang *et al.* 2008).

The cadherin/catenin system typically comprises N-cadherin (N-cadh), p120 catenin (p120 ctn), α-N-catenin, and β-catenin (β-ctn). Such complexes participate in the formation and stability of synapses, the development of dendrites, and the dynamic regulation of synaptic plasticity

Received April 5, 2016; revised manuscript received May 22, 2016; accepted May 31, 2016.

Address correspondence and reprint requests to Gloria Patricia Cardona-Gómez, Universidad de Antioquia, Sede de Investigación Universitaria (SIU), Calle 62 # 52–59, Torre 1, Piso 4, Laboratorio 412, Medellín, Colombia. E-mail: patricia.cardonag@udea.edu.co

Abbreviations used: AD, Alzheimer's disease; CDK5, cyclin-dependent kinase 5; MWM, Morris water maze; NMDA, *N*-methyl-D-aspartate receptor; NTFs, neurofibrillary tangles; p120 ctn, p120 catenin; PSD95, post-synaptic protein 95; shCDK5miR, CDK5 RNA short hairpin based microRNA-based; shSCRmiR, scrambled RNA short hairpin based microRNA-based; α-N-ctn, α-N-catenin; βA, β-amyloid; β-ctn β-catenin.

(Togashi *et al.* 2002; Okamura *et al.* 2004; Troyanovsky 2005; Bozdagi *et al.* 2010). The p120 ctn protein displays a pivotal role in cadherin complex stabilization and dendritic spine modulation (Davis *et al.* 2003; Elia *et al.* 2006). In addition, our previous study shows that neuroprotection after ischemic injury in rats had been linked to p120 ctn functions (Cespedes-Rubio *et al.* 2010).

Excitotoxicity caused by increased intracellular calcium levels during Alzheimer's disease (AD) has been associated with the calpain-dependent cleavage of p35 to p25. CDK5 forms a complex with p25 increasing its half-life, thereby inducing CDK5 over-activation, which is correlated with AD pathogenesis (Patrick *et al.* 1998, 1999; Kusakawa *et al.* 2000). AD is the most common form of senile dementia; its main characteristics are the progressive loss of learning and memory, aberrant synaptic plasticity and decrease in the number of neurons, synapses and dendritic spines (Reitz *et al.* 2011; Kulkarni and Firestein 2012; Sheng *et al.* 2012; Reitz and Mayeux 2014). The progressive accumulation of β-amyloid (βA) contained in senile plaques and hyperphosphorylated Tau forming neurofibrillary tangles (NTFs) has been described as the main histopathological hallmarks involved in AD progression (Bancher *et al.* 1989; Giannakopoulos *et al.* 2003; De Strooper *et al.* 2010; Iqbal *et al.* 2010). The p25/CDK5 complex has been implicated in the increased rate of Tau phosphorylation, being a good pharmacological/molecular target for AD (Baumann *et al.* 1993).

Our previous studies have shown that CDK5 silencing decreased Tau hyperphosphorylation and alleviated memory impairment in the 3xTgAD mouse model, which developed βA plaques and NTFs (Piedrahita *et al.* 2010; Castro-Alvarez *et al.* 2014). However, the role of different synaptic adhesion proteins regulated by CDK5, such as the cadherin/catenin system, in AD is still incomplete. In this study, we detected a reduction of p120 ctn expression in the brain of AD patients. We also evaluated how key synaptic proteins, such as N-cadherin, β-ctn, PSD95, and GluN2B might be modified in the 3xTgAD mouse model after learning and memory tasks. We also examined the effects of CDK5 silencing on those synaptic proteins and the contribution of p120 ctn in the CDK5 silencing-induced neuroprotection.

Materials and methods

Human brain samples

All individuals or relatives provided written informed consent for research, and this study was approved through the local ethical standards committee on human experimentation. We included seven cases of Sporadic Alzheimer Disease and six control cases obtained from the University of Antioquia Brain Bank (Table 1). For biochemical analysis, we used frozen samples obtained from the temporal cortex.

CDK5 RNAi design

RNAi sh-miR sequence for CDK5 silencing (shCDK5miR) and a control scrambled RNA sequence (shSCRmiR) was based on previously published sequences (Chang *et al.* 2006; Piedrahita *et al.* 2010). These sequences were cloned into human miR-30-based stem loops via polymerase-mediated extension of overlapping DNA oligonucleotides. For subcloning of the RNAi sequence into an adeno-associated viral vector (AAV), the following primers were used: shCDK5miR forward primer, 5′-AAAACTCGAGTGAG CGCTGACCAAGCTGCCAGACTATACTG TAAAGCCACAGA TGGG-3′, and reverse primer, 5-AAAAACTAGTAG GCGTT GACCAAGCTGCCAGACTATACCCATCTGTGGCTTTACAG-3′; shSCRmiR forward primer, 5-AAAACTCGAGTGAGCGCACC ATCGA ACCGTCAGAGTTACTGTAAAGCCACAGATGGG-3, and reverse primer, 5-AAAAACTAGTAGGCGTACCATCGAA CCGTCAGAGTTACCCATCTGTG GCTTTACAG-3′. The extension products were digested with XhoI and SpeI for directional cloning into a U6 expression plasmid (Boudreau *et al.* 2008).

Table 1 Clinical and neuropathological data for the AD patients from whose brain material was analyzed

Diagnostic	Gender	Age of onset	Age of death	Post-mortem index (h)	Braak NF stage	NIA-RI	CERAD score
SAD	F	82	92	5.5	VI	3	C
SAD	F	65	74	2.5	IV	3	C
SAD	F	69	76	3.75	VI	3	C
SAD	M	NA	83	4.3	VI	3	C
SAD	F	NA	85	2.8	V	3	C
SAD	M	78	86	6.3	IV	3	C
SAD	F	68	82	3.8	VI	3	C
Control	F	Nap	43	> 24	0	0	0
Control	M	Nap	60	> 24	0	0	0
Control	F	Nap	60	> 24	1	0	0
Control	F	Nap	84	4.3	2	1	A
Control	F	Nap	67	3.8	0	0	0
Control	F	Nap	75	14.4	0	0	0

AD, Alzheimer's disease; NA, not available; Nap, not applicable; NF, neurofibrillary.

Viral particle production

To produce AAV particles, we employed the large-scale production of heterologous proteins using Sf9 insect cell culture to co-infect recombinant baculovirus derived from the *Autographa californica* nuclear polyhedrosis virus (Urabe *et al.* 2002). The mouse U6 promoter-driven shCDK5miR and shSCRmiR expression cassettes were cloned into pAAV.CMV.hrGFP, which contains AAV serotype 2/5 inverted terminal repeats, and a CMV-humanized Renilla GFP (hrGFP)-simian virus 40 poly(A) reporter cassette (Urabe *et al.* 2002; Boudreau *et al.* 2009). The AAV titers were determined using quantitative PCR and/or DNA slot blot analysis. The AAV samples were dialyzed before use.

Animal procedures

A total of 10 homozygous 18- to 20-month-old 3xTg-AD and 10 18- to 20-month-old control mice, were randomly selected, keeping a similar proportion between male and female, with a median weight of 28 g (24–32 g) (Oddo *et al.* 2003). These mice were obtained from our in-house specific pathogen-free colony at the vivarium of SIU, University of Antioquia, Medellín, Colombia, and were maintained on a 12 : 12-h dark:light cycle; food and water were provided *ad libitum*. All of the animal procedures were performed in concordance with the ARRIVE guidelines. The animals were handled according to Colombian standards (Law 84/1989 and Resolution 8430/1993) and the NIH animal welfare care guidelines (Public Law 99–158, November 20, 1985, 'Animals in Research'). The $Cdk5^{+/+}$, $Cdk5^{+/-}$, and $Cdk5^{-/-}$ mice handling and care protocols were approved by the Bioethics Committee of the Faculty of Science of the University of Chile. Special care was taken to minimize animal suffering and to reduce the number of animals used.

The non-transgenic (non-Tg) and 3xTgAD animals were anesthetized [ketamine (5%) and xylazine (2%) to 50 mg/5 kg body weight] and bilaterally injected with 1 μL of AAV2-shSCRmiR (shSCRmiR) or AAV2-shCDK5miR (shCDK5miR) into both hippocampi (−1.7 anteroposterior, 0.8 (right) and −0.8 (left) lateral, and 3 mm dorsoventral to Bregma). The injections were performed using a 10-μL Hamilton syringe at a rate of 0.1 μL/min, and the syringe was withdrawn 5 min after the end of infusion. The experimental groups, consisting of 18- to 20-month-old non-Tg control mice and 3xTg-AD mice, were stereotaxically injected with shSCRmiR or shCDK5miR, respectively, and were evaluated 1 month post-injection (Fig. 2a). These procedures were performed based on our previous studies (Piedrahita *et al.* 2010; Castro-Alvarez *et al.* 2014).

Morris water maze test

A total of 10 3xTgAD mice and 10 control mice were subjected to the Morris water maze (MWM) test. A white plastic tank 1 m in diameter and 30 cm in height was filled with water (22 ± 2°C) to a depth of 20 cm. The platform (7 cm in diameter) was positioned at 1.5 cm below the surface of the water during spatial learning and 1.5 cm above the surface of the water during the visible test. The extramaze visual cues were placed around the room and remained in a fixed position throughout the experiment. Each session consisted of four successive trials (30-s intertrial intervals), and each trial was initiated by pseudorandomly placing the mice in one of four starting locations. The animals had been trained to remain on the platform for 30 s before the initial trial was performed. The latency to reach the platform was evaluated using a visible platform to control for differences in visual-motor ability or motivation between the experimental groups. Eight training sessions (four trials per session) using a hidden platform were conducted to examine spatial learning performance. When a mouse did not locate the platform after a maximum of 60 s, the animal was gently guided to the platform. The animals were allowed 48 h of retention time and were subsequently tested in a probe trial of spatial reference memory for 60 s in the absence of the platform. The latency to reach the exact former platform location and the number of crosses of the platform site were recorded during the probe trial.

The transfer test involved changing the platform position to another location in the pool and repeating the training sessions using the hidden platform (in the transfer test, only four sessions were performed). The probe trial was performed in the same manner as described for the initial MWM test (Fig. 2a). An automated system (Viewpoint, Lyon, France) was used to record the behavior of the mice.

CDK5 KO mice

$Cdk5^{+/+}$, $Cdk5^{+/-}$, and $Cdk5^{-/-}$ mice were generated as previously reported (Ohshima *et al.* 1996). Cortices were isolated from E18–E19 embryos and homogenized for western blot analysis.

Primary neuronal cultures

Primary neuronal cultures were prepared from pregnant Wistar rats at E18–E19. Hippocampal and cortical cultures were dissected, trypsinized, dissociated (Oddo *et al.* 2003), and cultured on multiwell plates pre-coated with poly-L-lysine (Sigma-Aldrich, St. Louis, MO, USA) in Neurobasal medium (Gibco, Rockville, MD, USA) containing B-27 supplement (Sigma-Aldrich), albumin from chicken egg white (Sigma-Aldrich), N2 human supplement (Gibco), and a penicillin–streptomycin antibiotic mixture (Gibco) at 37°C in a humidified atmosphere containing 5% CO_2 for a maximum of 19 days *in vitro* (DIV19). The primary cultures at DIV7 were transduced with 2 μL of AAV 2/5 (10 genomes per mL) at a 10^{12} titer for 3 h at 37°C. The transductions were kept for 12 days before administration of glutamate and inhibitor treatments. Isolated primary neurons were plated at a low density (52 cells/mm^2) for immunofluorescence analysis or at a high density (1500 cells/mm^2) for western blot.

p120 ctn RNAi

Mouse p120 ctn shRNA (m) and control shRNA lentiviral particles were synthesized by Santa Cruz Biotechnology, Inc. To knock down gene expression, p120 ctn shRNA (m) viral particles containing target-specific constructs encoding a 19–25 nt (short hairpin) shRNA were designed. Commercial control shRNA viral particles encoding a scrambled shRNA sequence that does not specifically degrade any known cellular mRNA were also used. At DIV12, primary neuronal cultures plated in 6- and 24-well plates were transduced for 7 days with 5 or 0.5 μL of lentiviral particles, respectively, at a titer of 10^6 infectious units of virus in Dulbecco's modified Eagle's medium containing 25 mM HEPES, pH 7.3.

Cell treatments

On DIV18, neurons were treated with 125 μM glutamate (Sigma-Aldrich) for 20 min (Urabe *et al.* 2002). After 24 h, the proteins

were collected, or the cells were fixed. To examine the neuronal effects of roscovitine on DIV18, neurons were treated with 10 μM roscovitine (Calbiochem, San Diego, CA, USA) or with dimethyl sulfoxide (0.01%) prepared in medium. Roscovitine was applied during the 24 h following glutamate excitotoxicity.

Cell transfections

HEK293T cells were transiently transfected with LZRS-empty-eGFP or LZRS-p120ctn-eGFP (provided by Albert B. Reynolds, Vanderbilt University School of Medicine, USA) in Opti-MEM with Lipofectamin 2000 (Invitrogen, Carlsbad, CA, USA). After 4 h, transfection medium was changed for Dulbecco's modified Eagle's medium + 10% Fetal Bovine Serum, and cells were lysed to protein analyses. Also, hippocampal neurons were transiently transfected with LZRS-empty-eGFP or LZRS-p120ctn-eGFP using Lipofectamine 2000 (Invitrogen) in neurobasal medium at DIV5. The neurons were transfected with 0.4 μg of DNA using Lipofectamine 2000 in 24-well culture plates at a density of 5.0×10^6 cells per well. After 4 h, the transfection medium was replaced with supplemented neurobasal medium. On DIV 7, the neurons were treated with 125 μM glutamate (20 min) to induce excitotoxicity. After glutamate treatment, the neurons were treated with 10 μM of roscovitine (Ros) for 24 h. On DIV8, the neurons were fixed and permeabilized for immunofluorescence analysis. A total of 60 eGFP-positive neurons from at least three independent experiments were used for nuclear quantification.

Western blotting

After behavioral testing, the animals were killed. The hippocampus was dissected, immediately frozen in liquid nitrogen, and stored at −80°C until use. Additionally, the neuronal cultures were collected after treatment, and human samples were stored at −80°C. All samples were lysed in 10 mM Tris, pH 7.4, 100 mM NaCl, 1 mM EDTA, 1 mM EGTA, 10% glycerol, 1% NP-40, 1 nM Na_3VO_4, 5 mM NaF, 1 mM phenylmethylsulfonyl fluoride and a protease inhibitor cocktail (Sigma-Aldrich) (Cardona-Gomez *et al.* 2004). A 30- to 40-μg aliquot of protein was mixed with loading buffer containing 0.375 M Tris (pH 6.8), 40% glycerol, 8% sodium dodecyl sulfate (SDS), 0.1 M dithiothreitol, and 0.002% bromophenol blue. Subsequently, the proteins were loaded on an 8% or 10% polyacrylamide gel and transferred to nitrocellulose membranes (GE Healthcare, Pittsburgh, PA, USA) at 250 mA for 2 h using an electrophoretic transfer system. The membranes were incubated overnight at 4°C in one of the following antibodies: anti-CDK5 (C-8) (rabbit); anti-p35/p25 (rabbit) (Santa Cruz Biotechnology, Santa Cruz, CA, USA); anti- GluN2B (rabbit); anti-PSD95 (mouse) (Merck Millipore, Darmstadt, Germany); anti-p120 catenin (mouse); anti-α-N-catenin (rabbit) (Sigma-Aldrich); anti-N-cadherin (mouse); anti-β-catenin (mouse) (Becton-Dickinson, Franklin Lakes, NJ, USA); or anti-βIII tubulin (mouse) (Promega, Madison, WI, USA). IRDye 800CW goat anti-mouse or anti-rabbit and 680CW goat anti-mouse or anti-rabbit (LI-COR, Inc. Lincoln, NE, USA) were used as the secondary probe. The blots were developed using the Odyssey Infrared Imaging System.

Immunoprecipitation

The PSD95 protein was immunoprecipitated from 200 μg of protein. The extracts were incubated overnight at 4°C under constant agitation in 1 μg of the primary antibody (mouse anti-PSD95; Calbiochem). A total of 30 μg of protein G sepharose (Sigma-Aldrich) was added, and the mixture was incubated for 4 h at 4°C. The protein G sepharose beads were washed five times with IP buffer (Sigma-Aldrich) at 4°C. After the fifth wash, 12.5 μL of SDS–polyacrylamide gel electrophoresis loading buffer (0.375 M Tris (pH 6.8), 40% glycerol, 8% SDS, 0.1 M DTT, and 0.002% bromophenol blue) was added, and the mixture was immediately incubated for 5 min at 95°C. The samples were electrophoretically separated on 8% polyacrylamide gels, and subsequently transferred to nitrocellulose membranes (GE Healthcare) at 250 mA for 2 h using an electrophoretic transfer system. The membranes were incubated overnight at 4°C in one of the following antibodies: anti-GluN2B (rabbit); anti-PSD95 (mouse) (Merck Millipore); anti-p120 ctn (mouse) (Sigma-Aldrich); anti-N-cadherin (mouse); or anti-β-catenin (mouse) (Becton-Dickinson). IRDye 800CW goat anti-mouse or anti-rabbit or IRDye 680CW goat anti-mouse or anti-rabbit (LI-COR, Inc.) were used as the secondary probe. The blots were developed using the Odyssey Infrared Imaging System. The results were normalized to the loading control values. The IgG peptide (1 : 100; Jackson Immuno-Research, West Grove, PA, USA) was used as an internal negative control for immunoprecipitation.

Immunofluorescence

The cultures were fixed in 4% paraformaldehyde prepared in cytoskeleton buffer for 20 min (Posada-Duque *et al.* 2013). Autofluorescence was blocked using 50 mM NH_4Cl. The cells were permeabilized and blocked with phosphate-buffered saline containing 0.1% Triton X-100 and 1% fetal bovine serum for 1 h. The cultures were incubated overnight at 4°C in the mouse anti-p120 ctn primary antibody (Sigma, St Louis, MO, USA). The Alexa 594 fluorescent secondary antibody was used (1 : 1000; Molecular Probes, Eugene, OR, USA). The nuclei were stained with Hoechst 33258 (1 : 5000; Invitrogen). The neurons were washed four times with buffer, coverslipped using Gel Mount (Biomeda, Foster city, CA, USA), and observed under an Olympus (Olympus, Tokyo, Japan) IX 81 epifluorescence or a DSU Spinning Disc Confocal microscope (Olympus, Tokyo, Japan). No staining was observed when the primary antibody was omitted.

Image processing

Images in the XY plane were collected using an Olympus IX 81 epifluorescence microscope equipped with a 60× (NA, 1.42) oil-immersion objective. Z-stack (6–10 optical sections) images were collected at 0.4-μm intervals encompassing the partial dendritic arbor using an Olympus IX 81 DSU Spinning Disc Confocal microscope equipped with a 60× oil-immersion objective (NA, 1.42). The image stacks were deconvoluted via a 3D-deconvolution algorithm following maximum intensity projection using Cell M imaging software (Olympus).

Quantitative image analysis

The percentage of condensed nuclei was calculated using the following formula: [condensed nuclei/(condensed nuclei + normal nuclei)] × 100. The mean area and diameter of each nucleus were quantified using the automated measurement/spatial trace tool. Condensed nuclei were defined as those displaying an average area

less than or equal to 40 μm^2 and a diameter less than or equal to 6 μm. The condensed nuclei were quantified in five 40× fields. The p120 ctn fluorescence intensity was determined using maximal projection images from Z stacks. The p120 ctn fluorescence intensity in the soma and the dendrites was obtained in eGFP-positive neurons. Also, p120 ctn intensity was determined in primary, secondary, and tertiary neurites using ROI for each neuron. A primary neurite was defined as an extension sprouting directly from the cell body with a minimum length of 1.5 times the length of the soma of the neuron; secondary neurites were neurites that emerged from the primary neurite and tertiary neurites were processes sprouting from secondary neurites. All of the dendrites of a single neuron were traced manually using the manual measurement/spatial trace feature tool. At least 15 neurons were quantified per independent assay. Because all fluorescence intensity measurements were obtained in the red and blue channels, the intensity of the color pixels was quantified as the fluorescence intensity. For each measurement of intensity, the field background was subtracted, and comparisons with the results of parallel experiments were performed (Piedrahita *et al.* 2010). Measurements were performed using Image Pro Plus software (Media Cybernetics, Rockville, MD, USA); 15 neurons were examined per treatment in duplicate assays of at least four independent experiments ($n = 4$).

LDH release

Cytotoxicity was assessed after measuring lactate dehydrogenase (LDH) release from the cultures using a cytotoxicity detection kit (Roche Molecular Biochemicals, Indianapolis, IN, USA). The culture medium was recovered 1 day after drug treatment (DIV19). LDH activity was determined by measuring the NADH absorption using a spectrophotometer to determine the linear rate of NADH consumption during the reduction of pyruvate to lactate. The percentage of cytotoxicity was calculated for a given test condition using the following equation: cytotoxicity (%) = [(A − low control)/(high control − low control)] × 100, where A represents the mean LDH activity in the media from three wells per duplicate of the given test conditions, low control represents LDH release from the untreated control cells, and high control represents the maximal LDH release from the cells (treated with 1% Triton X-100 for 24 h).

Rac and RhoA activation assays

A Rac and RhoA GTP enzyme-linked immunosorbent assay kit (Cytoskeleton; Biochem, Denver, CO, USA) was used to measure the Rac and RhoA activities following the protocol as we previously published in Posada-Duque *et al.* 2013; and according to the manufacturer's protocol.

Statistics

At least 3–4 mice were used for biochemical studies, 10 animals were used for behavioral evaluation, six controls, and seven AD brain samples were used for analysis and 3–5 samples were used for *in vitro* experiments. The parametric data for two groups were compared using Student's *t*-test, and non-parametric data were evaluated using the Mann–Whitney *U*-test. One-way ANOVA followed by Tukey's test for post hoc analysis was used to compare parametric data between four groups. The non-parametric data were evaluated using the Kruskal–Wallis test followed by Dunnett's post hoc test. The escape latency during the hidden platform training sessions was determined using repeated-measures ANOVA. One-way ANOVA was used to analyze the latency and the number of platform crosses in the hidden platform trials and in the probe trials. SPSS software was used. The values were expressed as the means ± SEM. The results were considered to be significant at $^{*,\#,+}p < 0.05$, $^{**,\#\#,++}p < 0.01$, and $^{***,\#\#\#,+++}p < 0.001$. All of the sample groups were processed in parallel to reduce interassay variation.

Results

Reduction of p120 ctn and related proteins as N-cadh and β-ctn were detected in human AD brains

An analysis of cadherin/catenin complex and synaptic proteins in sporadic AD brains revealed that the p120 ctn, N-cadh, β-ctn protein levels were significantly decreased. In contrast, α-N-catenin was not modified. Also, GluN2B and PSD95 were slightly reduced in the temporal cortex compared with control brains (Fig. 1a and b). However, when we evaluated the co-immunoprecipitation of p120 ctn and GluN2B to PSD95, no change was found (Fig. 1c–e), suggesting a reduction in the total synaptic adhesion complex, but not their association.

Reversal learning was affected in 3xTgAD mice, but recovered by CDK5 silencing

Following the experimental design showed in the Fig. 2(a), data confirmed our previous observations (Castro-Alvarez *et al.* 2014), where the visible platform trials showed that the shSCRmiR and shCDK5miR-treated mice did not exhibit visual or motor alterations. In general, all mice reached the platform (Fig. 2b), two mice were excluded from the experiment because they showed motor or motivational disturbances (data not shown). Furthermore, during the hidden platform learning sessions, the escape latency of the mice did not significantly differ between any of the experimental groups (Fig. 2b). At 48 h after the final training trial, the platform was removed from the pool, and the animals were allowed to swim freely and search for the platform for 1 min. In this trial, the 3xTgAD mice treated with shSCRmiR showed a memory deficit, represented by an increase in the latency to reach the platform location and a reduction in the number of crosses on the platform location compared with the control mice (Fig. 2c). In addition, the 3xTgAD mice treated with shCDK5miR showed a similar behavior to the control mice, suggesting that this treatment prevented the AD-induced memory impairment (Fig. 2c). The 3xTgAD mice treated with shScrmiR exhibited a random swimming path during the probe trial, but the control mice and 3xTgAD mice treated with CDK5 RNAi swam close to the initial platform location (Fig. 2d and e). However, we did not find significant differences between the experimental groups.

During the transfer test, in which the platform position was changed, followed by repeated learning sessions and a probe

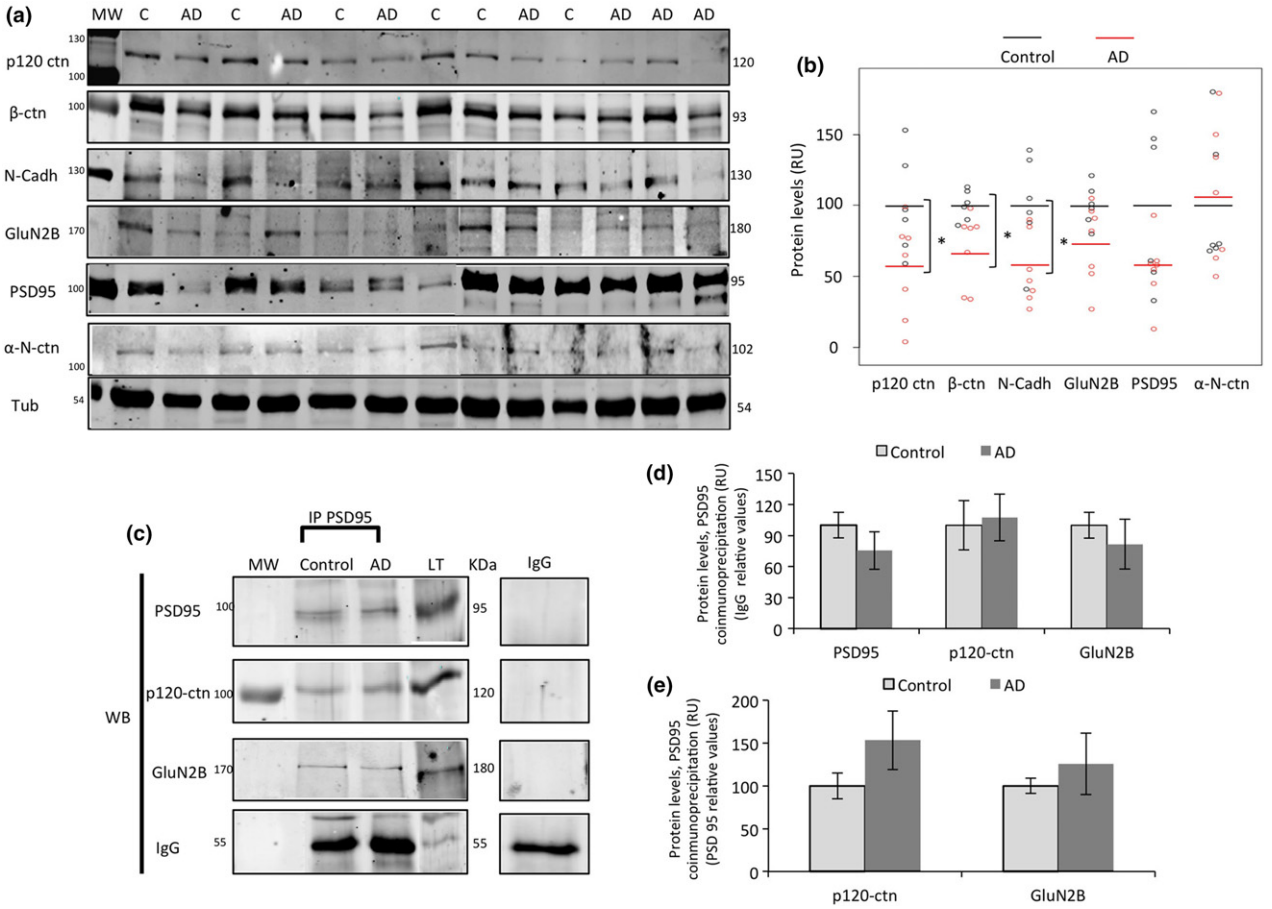

Fig. 1 p120 ctn and other synaptic adhesion proteins' deficiency was found in Alzheimer's disease brains. (a) Blots of p120 ctn, N-cadherin, β-catenin, α-N-catenin, GluN2B, and PSD95 from Alzheimer's disease brains. (b) Dot plot representing the quantification of each patient band shown in A. Tubulin was used as a loading control. (c) Representative blots of PSD95, GluN2B, and p120 ctn from the PSD95 immunoprecipitation assay. (d, e) Quantitative representation of the results shown in (c). The data were normalized to IgG load for evaluating changes in the complex (d) and relativized to PSD95 expression in order to detect variation in the association of the proteins (e). Densitometric quantification was performed. The data are presented as the means ± SEM (relative units). $n = 6–7$, $*p < 0.05$ (Student's t-test). MW, Molecular weight.

trial, we did not observe any differences between the experimental groups (Fig. 2f). However, the 3xTgAD mice treated with shSCRmiR exhibited a significantly higher escape latency (Fig. 2g), fewer crosses (Fig. 2h) and less time in the quadrant of the new platform location (Fig. 2i) compared with the control mice. Interestingly, we observed that CDK5 knockdown (KD) alleviated the memory deficit of 3xTgAD mice on the transfer test since the performance of this experimental group was similar to the control group (Fig. 2g–i). The swimming paths during the transfer test probe trial showed that the control mice and the 3xTgAD mice treated with shCDK5miR swam near the new platform location, but that the 3xTgAD mice treated with shSCRmiR exhibited a random swimming path (Fig. 2j). Treatment with shCDK5miR did not show any effect on the control mice (Fig. 2).

p120 ctn and related synaptic adhesion proteins collapse in 3xTgAD mice and were recovered under CDK5 knock-down condition

After the MWM test, we verified CDK5 silencing and GFP expression in the hippocampus of AAV-injected animals (Fig. 3a). As expected, CDK5 protein levels were reduced in the hippocampus of non-Tg and 3xTg AD mice treated with shCDK5miR (Fig. 3b and c). p35 and p25 protein levels did not show significant differences between groups (Fig. 3b and c). However, the 3xTgAD mice treated with the scrambled shRNA showed a significant increase in the p25/p35 ratio, which was reduced to control values by the shCDK5miR treatment (Fig. 3d).

Because of CDK5 targeting significantly preserving memory function, we determined the levels of synaptic adhesion proteins in 3xTgAD mice, and compared this with

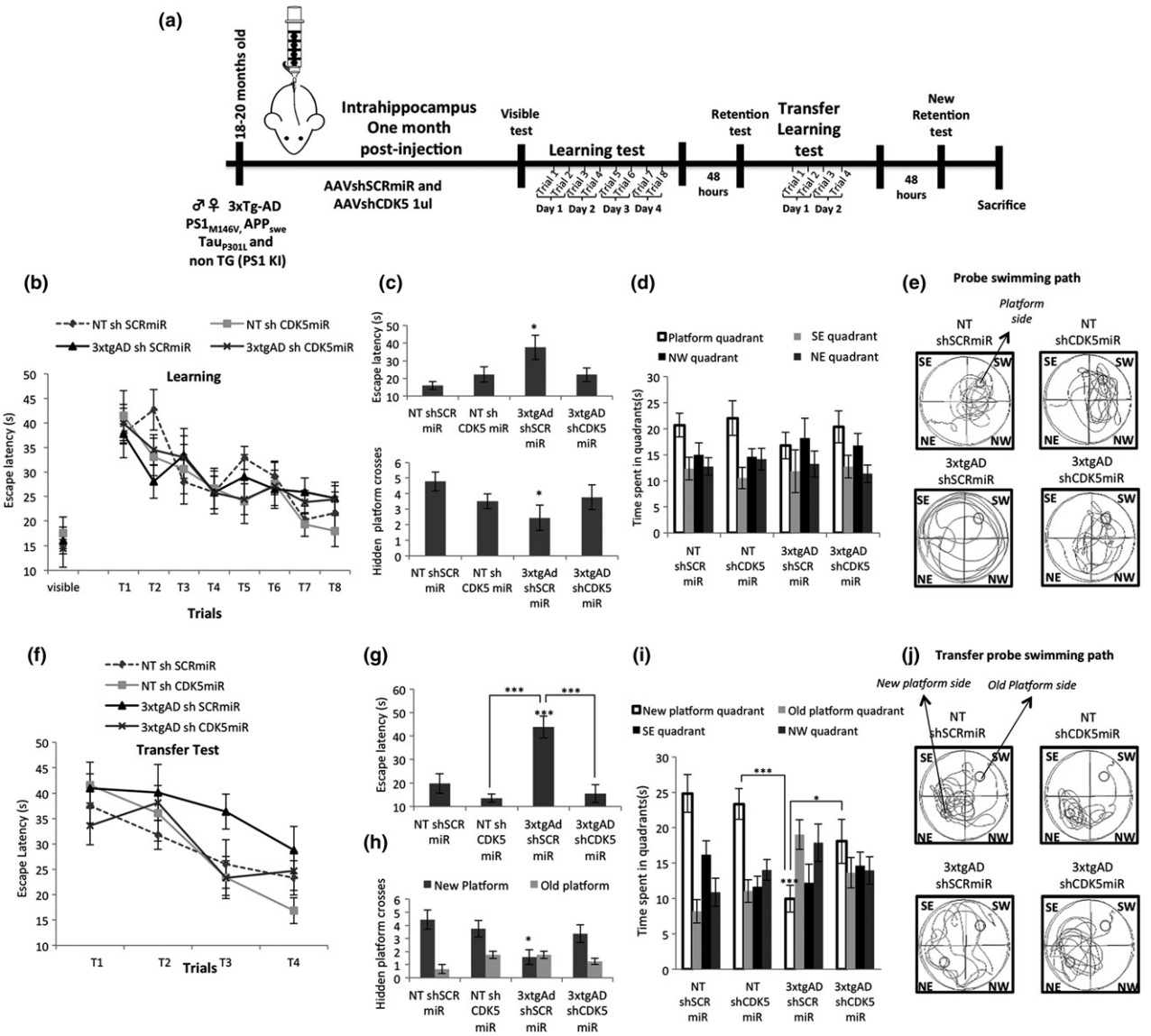

Fig. 2 CDK5 targeting protected the reversal learning performance of 3xTgAD mice. (a) Experimental design. AAVshSCRmiR and AAVshCDK5miR were injected in the hippocampus of 18–20-month-old Non-Tg and 3xTg-AD mice. One month post-injection, behavioral analysis using Morris water maze test were carried out following these steps: Day one, visible test was performed; next day, eight training sessions were conducted (4 days); 48 h thereafter, retention test was carried out. Afterward, the training transfer test was performed in only four sessions (2 days) followed by the new probe trial at 48 h. Finally, the mice were killed for biochemical analysis and some of them were fixed for checking the GFP expression. (b) There were no statistically significant differences in the latency to reach the hidden platform between any experimental groups during the learning test (two-way ANOVA followed by Dunnett's post hoc test for multiple comparisons). In the probe trial, which was performed 48 h after the final training trial, the 3xTgAD mice treated with shCDK5miR showed increased memory retention, as demonstrated by (c) an increased latency to reach the hidden platform and a reduced number of hidden platform crosses (Student's *t*-test comparing each experimental group with the control group. (d) There were no statistically significant differences in the time spent in the platform quadrant. (e) Representative swimming paths during the probe trial. (f) Statistically significant differences in the latency to reach the hidden platform were not observed between any experimental groups during the training sessions of the transfer test. (g) In the probe trial, performed 48 h after the final training session of the transfer test, the 3xTgAD mice treated with shCDK5miR showed a decreased latency to reach the hidden platform. (h) An increased number of crosses by the new hidden platform location, and (i) spent more time in the new platform quadrant location compared with 3xTgAD mice SCR version (ANOVA followed by Tukey's post hoc test). (j) Representative swimming paths during the transfer test. The data are presented as the means ± SEM. $n = 8$–10 for each group. $^*p < 0.05$, $^{***}p < 0.001$. SE, South-East; SW, South-West; NE, North-East; NW, North-West; AAV, adeno-associated viral vector.

results obtained from human brain samples. Interestingly, the protein levels of N-cadherin, p120 ctn, and β-ctn, in addition to GluN2B and PSD95 were significantly reduced in 3xTgAD mice treated with shSCRmiR compared with control mice. However, the N-cadherin/catenin system as well as GluN2B and PSD95 synaptic proteins was significantly recovered by the shCDK5miR treatment. Similar to the results obtained in human samples, no changes in α-N ctn were detected in any group (Fig. 3e and f).

N-cadherin/catenin post-synaptic adhesion complex was confirmed based on the PSD95 immunoprecipitation. Thus, p120 ctn, β-ctn, and GluN2B were associated to PSD95 and significantly reduced in the 3xTgAD mice compared with the control mice. Those reductions were recovered to control values by CDK5 silencing (Fig. 3g and h), when the precipitates were relativized with respect to the IgG load. However, there was no significant difference when arbitrary units were relativized to the PSD95 load (Fig. 3i), suggesting a reduction in the synaptic adhesion complex PSD95-dependent, but not their association.

p120 ctn is a target of CDK5 in neurites

To understand the relevance of p120 ctn on the CDK5 silencing-induced neuroprotection and synaptic plasticity, we used an *in vitro* excitotoxicity model induced by glutamate overload. p120 ctn protein level decreased because of glutamate excitotoxicity in total lysates (Fig. 4a and e), as did its fluorescence intensity in neurites (Fig. 4b and c). However, CDK5 silencing or a specific CDK5 inhibitor (Roscovitine) reversed such decrease, showing higher p120 ctn protein levels than the control values (Fig. 4a and e). Also, p120 ctn fluorescence intensity was recovered in neurites under CDK5 knockdown conditions (Fig. 4b and c), supported by scaling profile of p120ctn distribution on the neurons, which show a recovery of the p120 ctn in primary, secondary, and tertiary neurites by shCDK5miR after glutamate excitotoxicity (Fig. 4b and d). Interestingly, CDK5 silencing increased p120 ctn in primary and secondary neurites in basal conditions (without glutamate) (Fig. 4b and d). p120 ctn fluorescence intensity did not change in the soma for any treatment (Fig. 4b and c). Complementarily, we confirmed that the p120 ctn protein levels increased in both heterozygous and homozygous CDK5 KO mice (Fig. 4f). These results suggested that CDK5 regulates the p120 ctn protein levels and that the CDK5 protein reduction or its pharmacological inhibition may prevent p120ctn down-regulation.

shCDK5miR-induced neuroprotection requires p120 ctn

To determine the role of p120 ctn in neuroprotection, p120 ctn was knocked down in neurons exposed to glutamate, and previously silenced for CDK5. Neurons treated with glutamate showed increased LDH release, which was reversed by CDK5 silencing (Fig. 5a). Interestingly, shCDK5miR-induced neuroprotection was blocked by sh-p120ctn (Fig. 5a). Since p120ctn acts as a signal coordinator between cadherins and Rho-family GTPases to regulate cytoskeletal changes during neuroplasticity and survival, Rho GTPase activities were determined. Neurons treated with glutamate showed increased RhoA activity and decreased Rac activity (Fig. 5b), both of which were reversed after CDK5 silencing (Fig. 5b). Moreover, CDK5 shRNA-miR alone induced the up-regulation of active Rac (Fig. 5b). Interestingly, CDK5 shRNA-miR-induced neuroprotection was blocked by p120ctn shRNA. Under these conditions, there was an increased LDH release, increased RhoA activity, and decreased Rac activity (Fig. 5a and b). We confirmed that neurons transduced with shCDK5miR under basal and excitotoxic conditions showed increased p120 ctn protein levels and that these effects were blocked by sh-p120ctn (Fig. 5c). Subsequently, we analyzed the effect of p120 ctn over-expression on roscovitine-induced protection in neurons transfected with WT LZRS-p120ctn (Fig. 5d). First, we confirmed the previous observation that roscovitine exerted a neuroprotective effect on neurons exposed to glutamate (Fig. 5d and e). Furthermore, neuronal cultures transfected with LZRS-p120ctn, causing the over-expression of p120 ctn (Fig. 5f) showed decreased nuclear condensation in response to glutamate treatment (Fig. 5d and e). These data suggested that p120 ctn is necessary for neuroprotection and shCDK5miR-induced neuroprotection requires p120 ctn up-regulation.

Discussion

In this study, we provided significant evidence that p120 ctn is a potential target in AD models, as well as affected in sporadic AD human brains, and that the role of p120 ctn in neuroprotection and plasticity might be recovered by CDK5 silencing.

Several studies have suggested that the dysfunction of synapses and dendritic spines precedes neuronal dysfunction and death during AD-induced neurodegeneration (Chabrier *et al.* 2014; Mavroudis *et al.* 2014). These hypotheses are supported by evidence from studies examining various postmortem tissue samples obtained from AD patients, in which a loss of dendritic spines was clearly detected in the hippocampus and other brain areas associated with AD pathology (Knobloch and Mansuy 2008). The loss of dendritic spines has been shown in animal models of AD and has been associated with increased levels of hyperphosphorylated Tau and βA plaques, indicating that the loss of dendritic spines is an important event in cognitive impairment in murine AD models and in patients with AD (Bittner *et al.* 2010).

Under several pathological conditions, the function and regulation of PSD95 and the NMDA receptor subunit GluN2B is altered (Dau *et al.* 2014; Gan *et al.* 2014). These

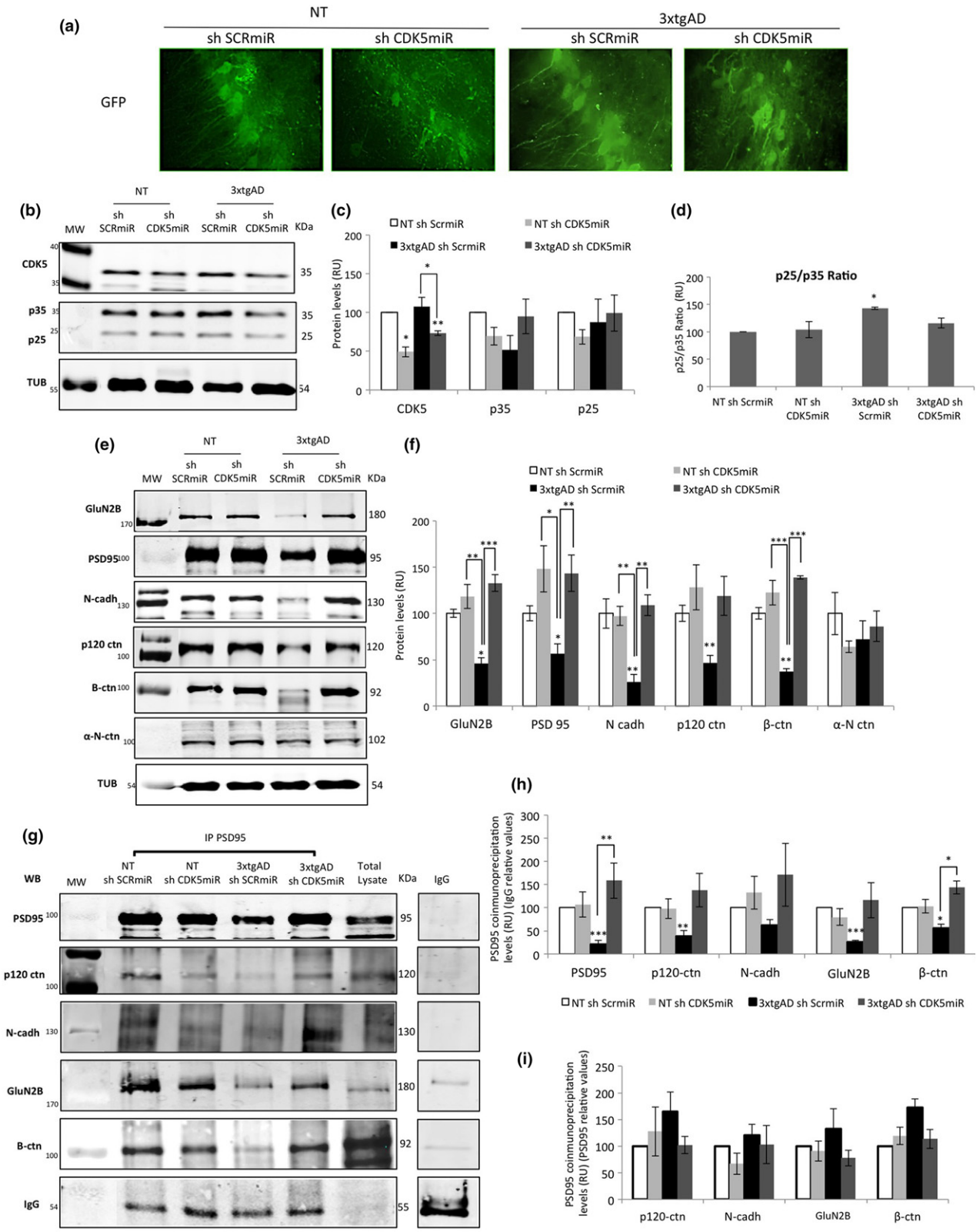

post-synaptic proteins have been implicated in synapse formation, neuronal plasticity, and cognitive functions such as memory and learning (Migaud *et al.* 1998; Craven *et al.* 1999; Brigman *et al.* 2010; Meyer *et al.* 2014a; Shipton and Paulsen 2014). The molecular dynamics of these proteins during memory and learning may be considered as markers

Fig. 3 The expression of p120 ctn and its related synaptic adhesion proteins was reduced in 3xTgAD mice and partially recovered by CDK5 silencing. (a) Representative GFP fluorescence from mice injected with adeno-associated viral vector (AAV)2-shSCRmiR or AAV2-shCDK5miR. Confocal images were captured at 60× magnification. Scale bar, 20 μm. The images shown are representative of four independent experiments. (b) Representative blots of the CDK5, p35 and p25 protein levels in 3xTgAD and control mice treated with shCDK5miR or shSCRmiR. (c) Quantitative representation of the results shown in (b). (d) The 3xTgAD mice showed an increased p25/p35 expression ratio, and this effect was reversed by CDK5 silencing. The synaptic and adhesion protein levels were decreased in the 3xTgAD mouse model, and CDK5 silencing ameliorated these effects. (e) Representative blots of N-cadherin, p120 catenin, β-catenin, α-N-catenin, GluN2B, and PSD95 in 3xTgAD and control mice treated with shCDK5miR or shSCRmiR. (f) Quantitative representation of the results shown in A. Tubulin was used as a loading control. Densitometric quantification was performed. (g) Representative blots of N-cadherin, p120 catenin, β-catenin, GluN2B, and PSD95 in the PSD95 immunoprecipitation assays. (h) and (i) Quantitative representation of the results shown in (g). Densitometric quantification was performed. The data were normalized to IgG load for analyzing changes in the complex expression (h) and relativized to PSD95 in order to evaluate the association between proteins (i) The data are presented as the mean relative units (RUs) ± SEM. $n = 3$–4. $^{*}p < 0.05$, $^{**}p < 0.01$, $^{***}p < 0.001$ (ANOVA followed by Tukey's post hoc test or the Kruskal–Wallis test followed by Dunnett's post hoc test, Student's *t*-test between experimental groups). MW, Molecular weight.

of synaptic function. GluN2B is decreased in the entorhinal and frontal cortices (Leuba *et al.* 2008), consistent with findings in AD human brains. However, in contrast to a tendency toward the reduction of PSD95 in the evaluated brains, an increase in PSD95 expression, accompanied by its altered distribution, has been previously described (Leuba *et al.* 2008, 2014; Sultana *et al.* 2010). This might reflect a differential tissue-specific expression of PSD95. Nevertheless, synaptic adhesion proteins such as, p120 ctn, N-cadh and β-ctn were weakly expressed in the temporal cortex of brain samples from human AD patients obtained following a short postmortem delay, and a stronger reduction was detected in the hippocampi of a 3xTgAD mice model together to a decrease of synaptic proteins such as GluN2B and PSD95. Those findings suggest that the N-cadherin/catenin complex could be affected by its attachment to synaptic proteins, which are involved in the synaptic failure that occurs during AD.

Complementarily, p120 ctn is a member of the cadherin/catenin complex, which plays an important role in the remodeling of dendritic spines, the maintenance of synaptic plasticity, and the regulation of the stability and dynamics of the N-cadherin/catenin system (Elia *et al.* 2006; Nanes *et al.* 2012). Consistent with these results, p120 ctn has been suggested as a part of the molecular pathway involved in the synaptic dysfunction associated with cognitive impairment in AD. The reduction in the p120 ctn protein levels in AD human brains was reproduced in the 3xTgAD mouse model, which exhibited memory performance impairment and significantly reduced synaptic adhesion complex levels. Interestingly, the loss of p120 ctn expression, primarily in neurites, was recapitulated in an *in vitro* glutamate-induced excitotoxicity model, supporting a role for p120 ctn in neuronal and synaptic plasticity. These results also suggest the potential relevance of p120 ctn protein in neurodegeneration.

On the other side, CDK5 hyperactivation is mediated by the cleavage of p35 to p25 conducting to hyperphosphorylated Tau accumulation (Ahlijanian *et al.* 2000; Kusakawa *et al.* 2000). This finding has been confirmed in this study and has been supported by previous reports showing the close correlation between CDK5 activity and the Tau phosphorylation state (Utreras *et al.* 2009; Piedrahita *et al.* 2010), the altered balance of kinases and phosphatases (Castro-Alvarez *et al.* 2015) and the over-stimulation of ion channels, which together promote the aggregation and formation of neurofibrillary tangles (Hou *et al.* 2013). Additionally, it has been previously shown that CDK5 silencing serves as a therapeutic strategy for AD (Lopez-Tobon *et al.* 2011) by ameliorating β-amyloidosis (Castro-Alvarez *et al.* 2015) reverting NTFs and alleviating or preventing memory performance alterations (Piedrahita *et al.* 2010; Castro-Alvarez *et al.* 2014). Consistently, the data obtained in this study showed that CDK5 down-regulation improved relearning performance in 3xtgAD mouse model, confirming the studies of our group and others to show that CDK5 reduction improves the reversal learning skills in Alzheimer′s mice model (Posada-Duque *et al.* 2015) and after cerebral ischemia in rats (Meyer *et al.* 2014b; Gutierrez-Vargas *et al.* 2015). However, we have not detected effects of shCDK5miR in the learning and memory function in old non-Tg mice (18 months) after 1 and 12 months post-injection (Castro-Alvarez *et al.* 2014), unlike to the experiments using conditional CDK5 KO mice, which showed improved MWM task performance on only the transfer test in younger mice (Hawasli *et al.* 2007), suggesting a differential modulation of CDK5 in adult brains in an age-dependent manner and under pathological conditions.

The transfer test evaluates reversal learning. During this phase of the MWM test, the results showed different electrophysiological implications where long-term depression plays a crucial role (Dong *et al.* 2013). In this sense, the described NMDA receptor, containing subunit GluN2A, is essential for the induction of Long Term Potentiation but not long-term depression; in contrast, the GluN2B subunit is essential for both processes (Paoletti *et al.* 2013). CDK5 regulates the degradation and subcellular distribution of GluN2B, and these phenomena have been implicated in

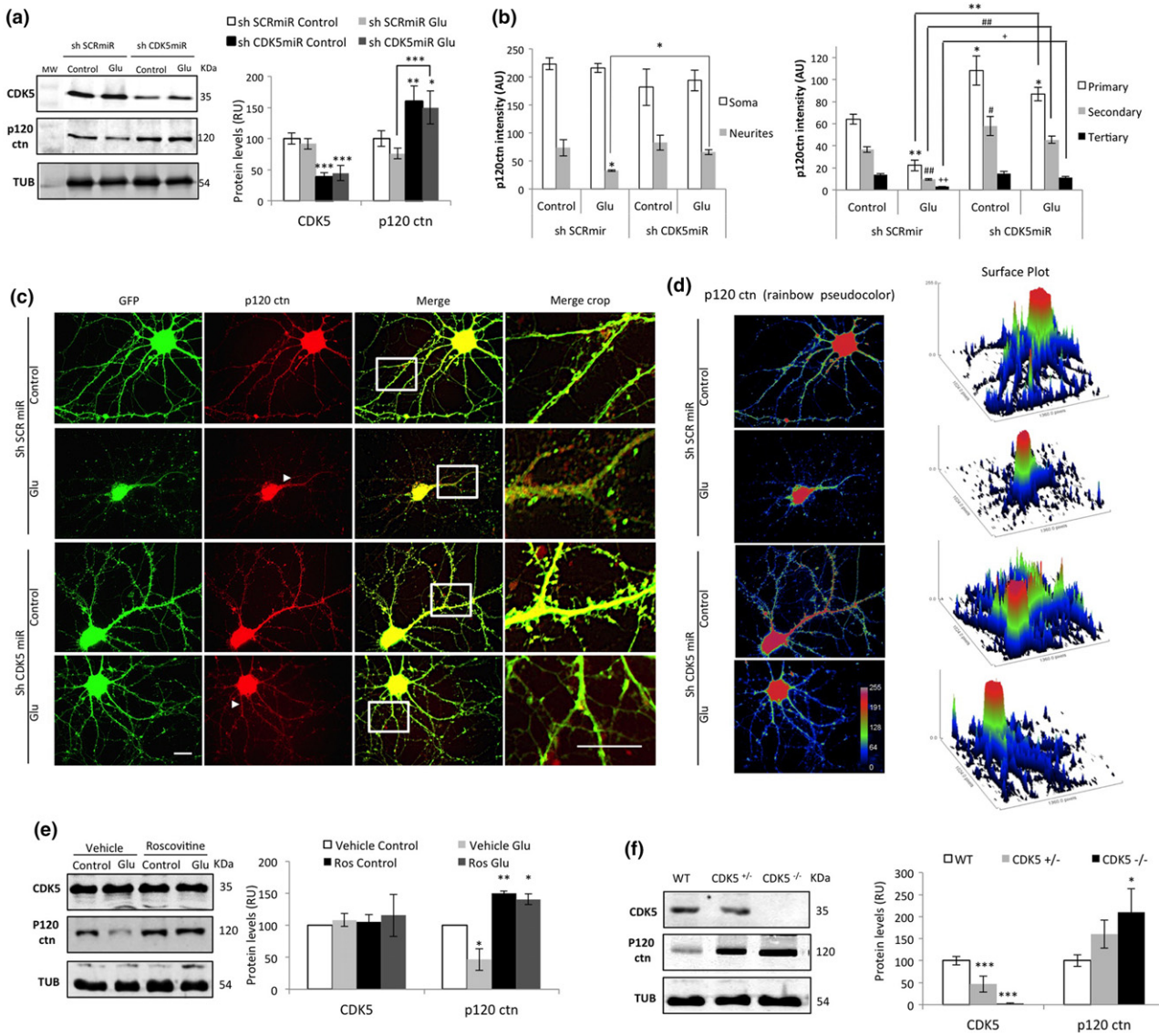

Fig. 4 p120 ctn is a target of CDK5 in neurites. The p120 ctn protein levels were decreased in the neurites of a glutamate-induced excitotoxicity model but were recovered by CDK5 silencing or roscovitine treatment. (a) Representative blots and quantitative representation of the CDK5 and p120 ctn levels in a glutamate-induced excitotoxicity model after CDK5 silencing. Tubulin was used as a loading control. Densitometric quantification was performed. The data are presented as the means ± SEM. $n = 3$, performed in duplicate. $^{*}p < 0.05$, $^{**}p < 0.01$, $^{***}p < 0.001$. (b) Relative units of fluorescence intensity from soma and dendrites were individually measured. p120 ctn intensity was determined in primary, secondary and tertiary neurites. Data are presented as the means ± SEM; $n = 5$, performed in duplicate. $^{*,\#,+}$ represent comparisons of p120 ctn intensity for primary, secondary and tertiary neurites, respectively. $^{*,\#,+}p < 0.05$, $^{**,\#\#,++}p < 0.01$; ANOVA with Tukey's test. (c) Neurons transduced with adeno-associated viral vector carrying eGFP-tagged SCR or CDK5 shRNA were immunostained for p120 ctn. Arrows: neurites formation; White squares: Merge crop. Confocal images were captured at 60× magnification. Scale bar, 20 μm. The images shown are representative of four independent experiments. (d) p120 ctn immunostaining rainbow pseudocolor representation and scaling intensity profile in a surface Plot. Signal Intensity is showed at the scale in bits. (e) Representative blots and quantitative graphs of the CDK5 and p120 ctn levels in a glutamate-induced excitotoxicity model after roscovitine treatment. Tubulin was used as a loading control. Densitometric quantification was performed. The data are presented as the means ± SEM. $n = 3$, performed in duplicate. $^{*}p < 0.05$, $^{**}p < 0.01$. The p120 ctn levels were increased in CDK5 KO mice. (f) Representative blots and quantitative representation of the CDK5 and p120 ctn protein levels in heterozygous and homozygous CDK5 KO mice. Tubulin was used as a loading control. Densitometric quantification was performed. The data are presented as the means ± SEM. $n = 3$, performed in duplicate. $^{*}p < 0.05$, $^{**}p < 0.01$ (ANOVA followed by Tukey's post hoc test or the Kruskal–Wallis test followed by Dunnett's post hoc test).

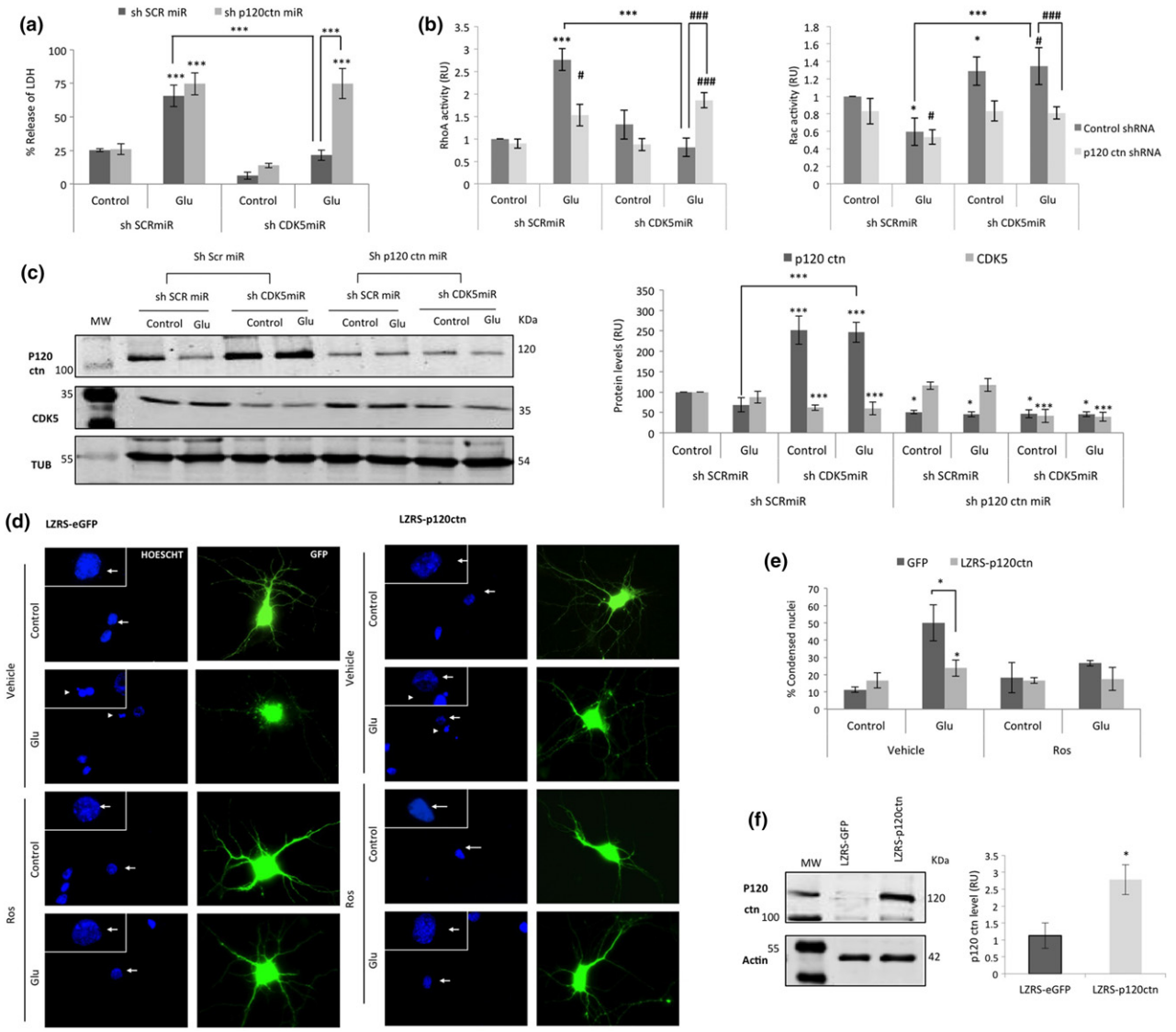

Fig. 5 Increased p120 ctn expression is necessary for CDK5 silencing-induced neuroprotection (a) CDK5 silencing-induced neuroprotection was reversed by p120 ctn knockdown. Neuronal cytotoxicity is presented as the percentage of lactate dehydrogenase release from the cells. The data are presented as the means ± SEM of three experiments performed in triplicate. p120 ctn over-expression protects against glutamate-induced cytotoxicity. Percentage of condensed nuclei relative to total nuclei in transfected neurons. (b) Rac and RhoA activity were quantified after 30 min of glutamate treatment as the amount of Rac-GTP and RhoA- GTP by ELISA (k = 490 nm). The data are presented as the means ± SEM from $n = 3$ per duplicate. Control shRNA: gray black bars and sh p120: gray light bars. * represents the comparison between each treatment of the control shRNA neurons or $^{\#}$ sh p120ctn neurons. * or $^{\#}p < 0.05$, *** or $^{\#\#\#}p < 0.001$; ANOVA with Tukey's test. (c) Representative blots and quantitative bars of the CDK5 and p120 ctn levels in a glutamate-induced excitotoxicity model and the respective controls after silencing both CDK5 and p120 ctn. Tubulin was used as a loading control. Densitometric quantification was performed. The data are presented as the means ± SEM. $n = 3$; each experiment was performed in duplicate. $^{*}p < 0.05$, $^{***}p < 0.001$. (d) Morphological characteristics are shown for neurons transfected with a plasmid expressing GFP-tagged (green) LZRS-eGFP or LZRS-p120ctn. The nuclei were stained with Hoechst (blue). The arrowhead shows the condensed nucleus for comparison with a normal nucleus (arrow). Magnification, 60×. Scale bar, 20 μm. (e) Graphic representation of the numerical results shown in (c). The data are presented as the means ± SEM of three experiments performed in duplicate. $^{*}p < 0.05$. (f) Representative blots and quantitation of the p120 ctn protein levels in HEK203T cells after LZRS-eGFP or LZRS-p120ctn transfection. Actin was used as a loading control. (ANOVA followed by Tukey's post hoc test or the Kruskal–Wallis test followed by Dunnett's post hoc test).

processes related to synaptic plasticity and cognition (Hawasli *et al.* 2007; Plattner *et al.* 2014). Additionally, the function and the distribution of PSD95 are regulated by the phosphorylation of its N-terminus via CDK5, this phosphorylation inhibits the multimerization of PSD95 and its anchoring to potassium channels (Morabito *et al.* 2004). These findings support that PSD95 and GluN2B down-regulation is associated with synaptic protein alterations and reduced MWM task performance in 3xTgAD mice and that amelioration of these effects in shCDK5miR-treated 3xTgAD mice potentially reflects the physiological dynamics of these synaptic proteins in neuroprotection (Morabito *et al.* 2004; Hawasli *et al.* 2007; Plattner *et al.* 2014). Therefore, the results of this study and previous studies suggest that targeting CDK5 over-activation not only prevents β-amyloidosis and tauopathy but also maintains synaptic protein homeostasis and promotes synaptic recovery.

Notably, p120 ctn also promotes Rac activation and RhoA inhibition, enhancing actin polymerization rate and the number of dendritic spines (Anastasiadis *et al.* 2000; Elia *et al.* 2006; Wildenberg *et al.* 2006). Similarly, p120 ctn regulates the stability and the endocytic rate of the cadherin/catenin system (Davis *et al.* 2003; Ouyang *et al.* 2013). Both mechanisms are associated with synapse formation and synaptic plasticity, and their alteration might result in neurodegenerative changes in AD. Interestingly, in this study, data showed that silencing, knocking out, or inhibiting CDK5 increases p120 ctn protein levels or recovers these levels in a degenerative context. It has been previously mentioned that dendritic localization and synaptic activity of δ-ctn, a homolog of p120 ctn, is regulated by CDK5-mediated phosphorylation (Poore *et al.* 2010). δ-ctn is phosphorylated by CDK5 in the ser 300 and ser 357 positions, inducing intracellular distribution. Furthermore, δ-ctn is associated with p35, and the loss of CDK5 activity generates its location in the membrane (Poore *et al.* 2010). In addition, p35, alone or in complex with CDK5, exerts neuroprotective effects in a Rac-dependent manner (Posada-Duque *et al.* 2015). Therefore, the silencing of CDK5 could produce an increase of the synaptic adhesion molecular complexes that include p120 ctn as part of the molecular mechanism involved in the synaptic function recovery and neuroprotection.

Also, we confirmed that CDK5 silencing induces the differential regulation of Rho GTPases, promoting Rac activity and suppressing RhoA activity (Posada-Duque *et al.* 2015). Active Rac1 is crucial for survival (Gutiérrez-Vargas *et al.* 2010), and RhoA is involved in neuronal death progression (Semenova *et al.* 2007). In addition, active Rac1 stimulates neurite outgrowth, synapse formation, and activity-dependent Ca^{2+} signals and it is regulated by p120 ctn (Elia *et al.* 2006; Linseman and Loucks 2008; Read and Gorman 2009). Complementarily, RhoA/ROCK signaling plays a central role in brain injury (Trapp *et al.* 2001; Semenova *et al.* 2007). The abnormal activity of CDK5/p25 and increased RhoA/ROCK activity associated with neurodegeneration suggest that the therapeutic effect of CDK5 silencing involves pro-survival signaling through the activation of Rac1 and the reversion of the active RhoA/ROCK, a pro-apoptotic pathway (Castro-Alvarez *et al.* 2011). Taken

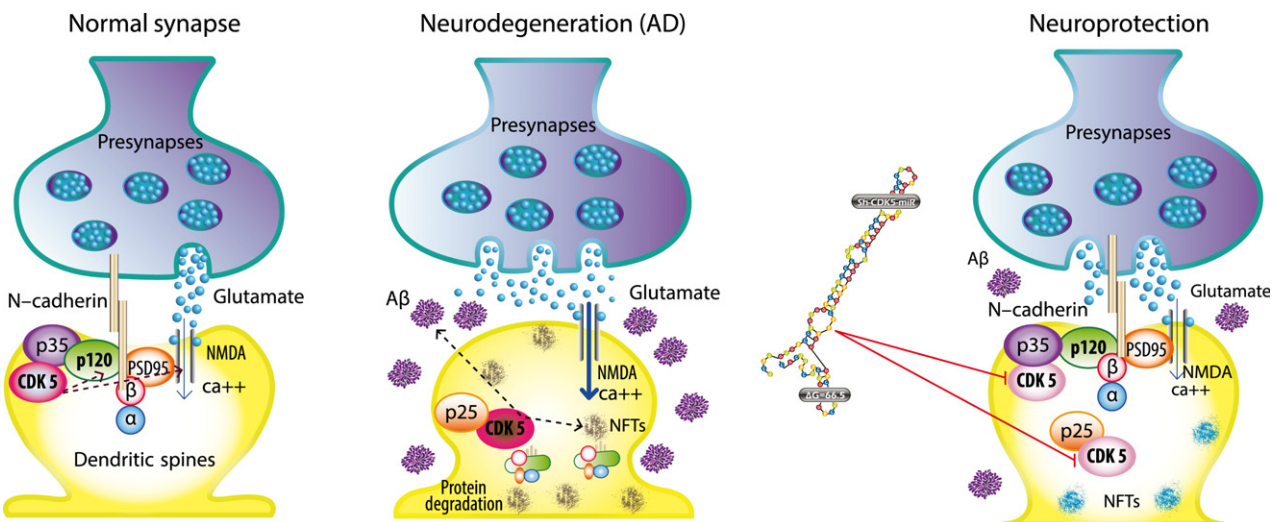

Fig. 6 Hypothetical scheme. p120 ctn underlying the neuroprotection depended on CDK5 Knock-down. p120ctn is part of the synaptic adhesion molecular complex (N-cadh/p120ctn/B-ctn/PSD95) modulated by the silencing of CDK5. During excitotoxicity and neurodegeneration, the p120ctn protein levels are affected together with PSD95 and recovered by the silencing of CDK5, because in agreement with our previous and current results, p120ctn is sustained in the cell membrane associated with p35, which is associated with neuroprotection and neuronal plasticity.

together, these data support the notion that CDK5 silencing modulates p120 ctn and RhoGTPases down-stream for inducing neuroprotection and plasticity.

In summary, our findings provide evidence that p120 ctn is reduced in sporadic AD human brains, p120 ctn plays an important role in the neuronal plasticity in *in vitro* and *in vivo* models of AD and contributes to the neuroprotection and prevention of memory dysfunction induced by CDK5 silencing (Fig. 6). Further studies are necessary for a better understanding of the relevance of the N-cadherin/Catenin system as a target in neurodegenerative processes and therapy.

Acknowledgments and conflict of interest disclosure

The authors thank the American Journal Experts for editing the English language in this manuscript, Yuliana Gomez for the graphical design, and Tania Marquez for assistance with the rat and mouse colonies at the specific pathogen-free vivarium. This research was financially supported by a grant from the Departamento Administrativo de Ciencia, Tecnología e Innovación, projects No. 111545921503 and No. 111554531400 (GPCG), Mobility's Project Colombia-Chile 576-2011 and the PROLAB Collaboration in Latin America/IBRO. In addition, this research was supported by the Fogarty International Center and the NIA of NIH under Award Number RO1-AG029802-01. CG-B is supported by CONICYT grants Fondecyt 1430325 and FONDAP 15150012. The authors thank the Advanced Microscopy Unit and Viral Vector and Gene Therapy Cores of the Group of Neuroscience of the University of Antioquia. The content of this manuscript is solely the responsibility of the authors and does not necessarily represent the official views of the National Institutes of Health. The authors declare no conflict of interest.

All experiments were conducted in compliance with the ARRIVE guidelines.

Supporting information

Additional Supporting Information may be found online in the supporting information tab for this article:

Figure S1. Full unedited gels for p120ctn, GluN2B, PSD95, N-Cadh, B-ctn, alpha-N-ctn from Figure 1a.

Figure S2. Full unedited gels for p120ctn, GluN2B, PSD95 from Figure 1c. DE: Data was excluided, NP: No protein, Mistake in the western blot Processing, TL: Total lysate.

Figure S3. Full unedited gels for CDK5, p35, p25, p120ctn, GluN2B, PSD95, N cadh, B-ctn from Figure 3b and 3e. Line 1–4 were excluded from the study, Line 5 NT sh SCR miR, Line 6 NT sh CDK5 miR, Line 7 3xtgAD SCR miR, Line 8 3xtgAD CDK5 miR.

Figure S4. Full unedited gels for p120ctn, GluN2B, PSD95, N cadh, B-ctn from Figure 3g. Line 1–4 were excluded from the study, Line 5 NT sh SCR miR, Line 6 NT sh CDK5 miR, Line 7 3xtgAD SCR miR, Line 8 3xtgAD CDK5 miR, Line 9 Total Lysates.

Figure S5. **A.** Full unedited gels for CDK5 and p120ctn from Figure 4a. Line 1 shSCRmiR + Vehicle, Line 2 shSCRmiR + Glutamate, Line 3 shCDK5miR + Vehicle, Line 4 shCDK5miR + Glutamate, Line 5 shSCRmiR + Vehicle, Line 6 shSCRmiR + Glutamate, Line 7 shCDK5miR + Vehicle, Line 8 shCDK5miR + Glutamate. (b) Full unedited gels for CDK5 and p120ctn from Figure 4e. Line 1 Vehicle, Line 2 Glutamate, Line 3 RoscoviQne, Line 4 Glutamate + RoscoviQne, Line 5 Vehicle, Line 6 Glutamate, Line 7 RoscoviQne, Line 8 Glutamate + RoscoviQne. (c) Full unedited gels for p120ctn from Figure 4f. Line 1 WT, Line 2 $Cdk5^{+/-}$, Line 3 $CDK5^{-/-}$. (d) Full unedited gels forCDK5 from Figure 4f. Line 1 and 2 $Cdk5^{+/-}$, Line 3 and 4 WT, Line 5 and 6 $CDK5^{-/-}$.

Figure S6. (a) Full unedited gels for CDK5 and p120ctn from Figure 5c. Line 1 Control shRNA + shSCRmiR + Vehicle, Line 2 Control shRNA + shSCRmiR + Glutamate, Line 3 Control shRNA + shCDK5miR + Vehicle, Line 4 Control shRNA + shCDK5miR + Glutamate, Line 5 p120ctn shRNA + shSCRmiR + Vehicle, Line 6 p120ctn shRNA + shSCRmiR + Glutamate, Line 7 p120ctn shRNA + shCDK5miR + Vehicle, Line 8 p120ctn shRNA + shCDK5miR + Glutamate. (b) Full unedited gels for p120ctn from Figure 5f. Line 1 LZRS-control, Line 2 LZRS-control, Line 3 LZRS-control, Line 4 LZRS-p120ctn, Line 5 LZRS-p120ctn, Line 6 LZRS-p120ctn, Line 7 LZRS-p120ctn, Line 8 LZRS-p120ctn.

References

Ahlijanian M. K., Barrezueta N. X., Williams R. D. *et al.* (2000) Hyperphosphorylated tau and neurofilament and cytoskeletal disruptions in mice overexpressing human p25, an activator of cdk5. *Proc. Natl Acad. Sci. USA* **97**, 2910–2915.

Anastasiadis P. Z., Moon S. Y., Thoreson M. A., Mariner D. J., Crawford H. C., Zheng Y. and Reynolds A. B. (2000) Inhibition of RhoA by p120 catenin. *Nat. Cell Biol.* **2**, 637–644.

Angelo M., Plattner F. and Giese K. P. (2006) Cyclin-dependent kinase 5 in synaptic plasticity, learning and memory. *J. Neurochem.* **99**, 353–370.

Bancher C., Brunner C., Lassmann H. *et al.* (1989) Accumulation of abnormally phosphorylated tau precedes the formation of neurofibrillary tangles in Alzheimer's disease. *Brain Res.* **477**, 90–99.

Baumann K., Mandelkow E. M., Biernat J., Piwnica-Worms H. and Mandelkow E. (1993) Abnormal Alzheimer-like phosphorylation of tau-protein by cyclin-dependent kinases cdk2 and cdk5. *FEBS Lett.* **336**, 417–424.

Bittner T., Fuhrmann M., Burgold S., Ochs S. M., Hoffmann N., Mitteregger G., Kretzschmar H., LaFerla F. M. and Herms J. (2010) Multiple events lead to dendritic spine loss in triple transgenic Alzheimer's disease mice. *PLoS ONE* **5**, e15477.

Boudreau R. L., Monteys A. M. and Davidson B. L. (2008) Minimizing variables among hairpin-based RNAi vectors reveals the potency of shRNAs. *RNA* **14**, 1834–1844.

Boudreau R. L., McBride J. L., Martins I., Shen S., Xing Y., Carter B. J. and Davidson B. L. (2009) Nonallele-specific silencing of mutant and wild-type huntingtin demonstrates therapeutic efficacy in Huntington's disease mice. *Mol. Ther.* **17**, 1053–1063.

Bozdagi O., Wang X. B., Nikitczuk J. S., Anderson T. R., Bloss E. B., Radice G. L., Zhou Q., Benson D. L. and Huntley G. W. (2010) Persistence of coordinated long-term potentiation and dendritic spine enlargement at mature hippocampal CA1 synapses requires N-cadherin. *J. Neurosci.* **30**, 9984–9989.

Brigman J. L., Wright T., Talani G. *et al.* (2010) Loss of GluN2B-containing NMDA receptors in CA1 hippocampus and cortex impairs long-term depression, reduces dendritic spine density, and disrupts learning. *J. Neurosci.* **30**, 4590–4600.

Cardona-Gomez P., Perez M., Avila J., Garcia-Segura L. M. and Wandosell F. (2004) Estradiol inhibits GSK3 and regulates interaction of estrogen receptors, GSK3, and beta-catenin in the hippocampus. *Mol. Cell Neurosci.* **25**, 363–373.

Castro-Alvarez J. F., Gutierrez-Vargas J., Darnaudery M. and Cardona-Gomez G. P. (2011) ROCK inhibition prevents tau hyperphosphorylation and p25/CDK5 increase after global cerebral ischemia. *Behav. Neurosci.* **125**, 465–472.

Castro-Alvarez J. F., Uribe-Arias S. A., Kosik K. S. and Cardona-Gomez G. P. (2014) Long and short-term CDK5 knockdown prevents spatial memory dysfunction and tau pathology of triple transgenic Alzheimer′s mice. *Front. Aging Neurosci.* **6**, 243.

Castro-Alvarez J. F., Uribe-Arias A. and Cardona-Gomez G. P. (2015) Cyclin-dependent kinase 5 targeting prevents beta-amyloid aggregation involving glycogen synthase kinase 3beta and phosphatases. *J. Neurosci. Res.* **93**, 1258–1266.

Cespedes-Rubio A., Jurado F. W. and Cardona-Gomez G. P. (2010) p120 catenin/alphaN-catenin are molecular targets in the neuroprotection and neuronal plasticity mediated by atorvastatin after focal cerebral ischemia. *J. Neurosci. Res.* **88**, 3621–3634.

Chabrier M. A., Cheng D., Castello N. A., Green K. N. and LaFerla F. M. (2014) Synergistic effects of amyloid-beta and wild-type human tau on dendritic spine loss in a floxed double transgenic model of Alzheimer's disease. *Neurobiol. Dis.* **64**, 107–117.

Chang K., Elledge S. J. and Hannon G. J. (2006) Lessons from nature: microRNA-based shRNA libraries. *Nat. Methods* **3**, 707–714.

Craven S. E., El-Husseini A. E. and Bredt D. S. (1999) Synaptic targeting of the postsynaptic density protein PSD-95 mediated by lipid and protein motifs. *Neuron* **22**, 497–509.

Dau A., Gladding C. M., Sepers M. D. and Raymond L. A. (2014) Chronic blockade of extrasynaptic NMDA receptors ameliorates synaptic dysfunction and pro-death signaling in Huntington disease transgenic mice. *Neurobiol. Dis.* **62**, 533–542.

Davis M. A., Ireton R. C. and Reynolds A. B. (2003) A core function for p120-catenin in cadherin turnover. *J. Cell Biol.* **163**, 525–534.

De Strooper B., Vassar R. and Golde T. (2010) The secretases: enzymes with therapeutic potential in Alzheimer disease. *Nat. Rev. Neurol.* **6**, 99–107.

Dong Z., Bai Y., Wu X. *et al.* (2013) Hippocampal long-term depression mediates spatial reversal learning in the Morris water maze. *Neuropharmacology* **64**, 65–73.

Elia L. P., Yamamoto M., Zang K. and Reichardt L. F. (2006) p120 catenin regulates dendritic spine and synapse development through Rho-family GTPases and cadherins. *Neuron* **51**, 43–56.

Gan J., Qi C., Mao L. M. and Liu Z. (2014) Changes in surface expression of N-methyl-D-aspartate receptors in the striatum in a rat model of Parkinson's disease. *Drug Des. Devel. Ther.* **8**, 165–173.

Giannakopoulos P., Herrmann F. R., Bussiere T., Bouras C., Kovari E., Perl D. P., Morrison J. H., Gold G. and Hof P. R. (2003) Tangle and neuron numbers, but not amyloid load, predict cognitive status in Alzheimer's disease. *Neurology* **60**, 1495–1500.

Gutierrez-Vargas J. A., Munera A. and Cardona-Gomez G. P. (2015) CDK5 knockdown prevents hippocampal degeneration and cognitive dysfunction produced by cerebral ischemia. *J. Cereb. Blood Flow Metab.* **35**, 1937–1949.

Gutiérrez-Vargas J. A., Castro-Álvarez J. F., Velásquez-Carvajal D., Montañez-Velásquez M. N., Céspedes-Rubio A. and Cardona-Gómez G. P. (2010) Rac1 activity changes are associated with neuronal pathology and spatial memory long-term recovery after global cerebral ischemia. *Neurochem. Int.* **57**, 762–773.

Hawasli A. H., Benavides D. R., Nguyen C. *et al.* (2007) Cyclin-dependent kinase 5 governs learning and synaptic plasticity via control of NMDAR degradation. *Nat. Neurosci.* **10**, 880–886.

Hou H., Sun L., Siddoway B. A., Petralia R. S., Yang H., Gu H., Nairn A. C. and Xia H. (2013) Synaptic NMDA receptor stimulation activates PP1 by inhibiting its phosphorylation by Cdk5. *J. Cell Biol.* **203**, 521–535.

Iqbal K., Wang X., Blanchard J., Liu F., Gong C. X. and Grundke-Iqbal I. (2010) Alzheimer's disease neurofibrillary degeneration: pivotal and multifactorial. *Biochem. Soc. Trans.* **38**, 962–966.

Knobloch M. and Mansuy I. M. (2008) Dendritic spine loss and synaptic alterations in Alzheimer's disease. *Mol. Neurobiol.* **37**, 73–82.

Ko J., Humbert S., Bronson R. T., Takahashi S., Kulkarni A. B., Li E. and Tsai L. H. (2001) p35 and p39 are essential for cyclin-dependent kinase 5 function during neurodevelopment. *J. Neurosci.* **21**, 6758–6771.

Kulkarni V. A. and Firestein B. L. (2012) The dendritic tree and brain disorders. *Mol. Cell Neurosci.* **50**, 10–20.

Kusakawa G., Saito T., Onuki R., Ishiguro K., Kishimoto T. and Hisanaga S. (2000) Calpain-dependent proteolytic cleavage of the p35 cyclin-dependent kinase 5 activator to p25. *J. Biol. Chem.* **275**, 17166–17172.

Kwon Y. T., Gupta A., Zhou Y., Nikolic M. and Tsai L. H. (2000) Regulation of N-cadherin-mediated adhesion by the p35-Cdk5 kinase. *Curr. Biol.* **10**, 363–372.

Lalioti V., Pulido D. and Sandoval I. V. (2010) Cdk5, the multifunctional surveyor. *Cell Cycle* **9**, 284–311.

Leuba G., Savioz A., Vernay A., Carnal B., Kraftsik R., Tardif E., Riederer I. and Riederer B. M. (2008) Differential changes in synaptic proteins in the Alzheimer frontal cortex with marked increase in PSD-95 postsynaptic protein. *J. Alzheimers Dis.* **15**, 139–151.

Leuba G., Vernay A., Kraftsik R., Tardif E., Riederer B. M. and Savioz A. (2014) Pathological reorganization of NMDA receptors subunits and postsynaptic protein PSD-95 distribution in Alzheimer's disease. *Curr. Alzheimer Res.* **11**, 86–96.

Linseman D. A. and Loucks F. A. (2008) Diverse roles of Rho family GTPases in neuronal development, survival, and death. *Front Biosci.* **13**, 657–676.

Lopez-Tobon A., Castro-Alvarez J. F., Piedrahita D., Boudreau R. L., Gallego-Gomez J. C. and Cardona-Gomez G. P. (2011) Silencing of CDK5 as potential therapy for Alzheimer's disease. *Rev. Neurosci.* **22**, 143–152.

Mavroudis I., Manani M., Petrides F., Petsoglou C., Njau S., Costa V. and Baloyannis S. (2014) Dendritic and spinal alterations of neurons from Edinger-Westphal nucleus in Alzheimer's disease. *Folia Neuropathol.* **52**, 197–204.

Meyer D., Bonhoeffer T. and Scheuss V. (2014a) Balance and stability of synaptic structures during synaptic plasticity. *Neuron* **82**, 430–443.

Meyer D. A., Torres-Altoro M. I., Tan Z. *et al.* (2014b) Ischemic stroke injury is mediated by aberrant Cdk5. *J. Neurosci.* **34**, 8259–8267.

Migaud M., Charlesworth P., Dempster M. *et al.* (1998) Enhanced long-term potentiation and impaired learning in mice with mutant postsynaptic density-95 protein. *Nature* **396**, 433–439.

Mishiba T., Tanaka M., Mita N., He X., Sasamoto K., Itohara S. and Ohshima T. (2014) Cdk5/p35 functions as a crucial regulator of spatial learning and memory. *Mol. Brain* **7**, 82.

Mita N., He X., Sasamoto K., Mishiba T. and Ohshima T. (2014) Cyclin-dependent kinase 5 regulates dendritic spine formation and maintenance of cortical neuron in the mouse brain. *Cereb. Cortex* **26**, 967–976.

Morabito M. A., Sheng M. and Tsai L. H. (2004) Cyclin-dependent kinase 5 phosphorylates the N-terminal domain of the postsynaptic density protein PSD-95 in neurons. *J. Neurosci.* **24**, 865–876.

Nanes B. A., Chiasson-MacKenzie C., Lowery A. M., Ishiyama N., Faundez V., Ikura M., Vincent P. A. and Kowalczyk A. P. (2012) p120-catenin binding masks an endocytic signal conserved in classical cadherins. *J. Cell Biol.* **199**, 365–380.

Oddo S., Caccamo A., Shepherd J. D. *et al.* (2003) Triple-transgenic model of Alzheimer's disease with plaques and tangles: intracellular A≤ and synaptic dysfunction. *Neuron* **39**, 409–421.

Ohshima T., Ward J. M., Huh C. G., Longenecker G., Veeranna Pant H. C., Brady R. O., Martin L. J. and Kulkarni A. B. (1996) Targeted disruption of the cyclin-dependent kinase 5 gene results in abnormal corticogenesis, neuronal pathology and perinatal death. *Proc. Natl Acad. Sci. USA* **93**, 11173–11178.

Okamura K., Tanaka H., Yagita Y., Saeki Y., Taguchi A., Hiraoka Y., Zeng L. H., Colman D. R. and Miki N. (2004) Cadherin activity is required for activity-induced spine remodeling. *J. Cell Biol.* **167**, 961–972.

Ouyang M., Lu S., Kim T. *et al.* (2013) N-cadherin regulates spatially polarized signals through distinct p120ctn and beta-catenin-dependent signalling pathways. *Nat. Commun.* **4**, 1589.

Paoletti P., Bellone C. and Zhou Q. (2013) NMDA receptor subunit diversity: impact on receptor properties, synaptic plasticity and disease. *Nat. Rev. Neurosci.* **14**, 383–400.

Patrick G. N., Zhou P., Kwon Y. T., Howley P. M. and Tsai L. H. (1998) p35, the neuronal-specific activator of cyclin-dependent kinase 5 (Cdk5) is degraded by the ubiquitin-proteasome pathway. *J. Biol. Chem.* **273**, 24057–24064.

Patrick G. N., Zukerberg L., Nikolic M., de la Monte S., Dikkes P. and Tsai L. H. (1999) Conversion of p35 to p25 deregulates Cdk5 activity and promotes neurodegeneration. *Nature* **402**, 615–622.

Piedrahita D., Hernandez I., Lopez-Tobon A. *et al.* (2010) Silencing of CDK5 reduces neurofibrillary tangles in transgenic alzheimer's mice. *J. Neurosci.* **30**, 13966–13976.

Plattner F., Hernandez A., Kistler T. M. *et al.* (2014) Memory enhancement by targeting Cdk5 regulation of NR2B. *Neuron* **81**, 1070–1083.

Poore C. P., Sundaram J. R., Pareek T. K. *et al.* (2010) Cdk5-mediated phosphorylation of delta-catenin regulates its localization and GluR2-mediated synaptic activity. *J. Neurosci.* **30**, 8457–8467.

Posada-Duque R. A., Velasquez-Carvajal D., Eckert G. P. and Cardona-Gomez G. P. (2013) Atorvastatin requires geranylgeranyl transferase-I and Rac1 activation to exert neuronal protection and induce plasticity. *Neurochem. Int.* **62**, 433–445.

Posada-Duque R. A., Lopez-Tobon A., Piedrahita D., Gonzalez-Billault C. and Cardona-Gomez G. P. (2015) p35 and Rac1 underlie the neuroprotection and cognitive improvement induced by CDK5 silencing. *J. Neurochem.* **134**, 354–370.

Read D. E. and Gorman A. M. (2009) Involvement of Akt in neurite outgrowth. *Cell. Mol. Life Sci.* **66**, 2975–2984.

Reitz C. and Mayeux R. (2014) Alzheimer disease: epidemiology, diagnostic criteria, risk factors and biomarkers. *Biochem. Pharmacol.* **88**, 640–651.

Reitz C., Brayne C. and Mayeux R. (2011) Epidemiology of Alzheimer disease. *Nat. Rev. Neurol.* **7**, 137–152.

Semenova M. M., Maki-Hokkonen A. M., Cao J., Komarovski V., Forsberg K. M., Koistinaho M., Coffey E. T. and Courtney M. J. (2007) Rho mediates calcium-dependent activation of p38alpha and subsequent excitotoxic cell death. *Nat. Neurosci.* **10**, 436–443.

Sheng M., Sabatini B. L. and Sudhof T. C. (2012) Synapses and Alzheimer's disease. *Cold Spring Harb. Perspect. Biol.* **4**.

Shipton O. A. and Paulsen O. (2014) GluN2A and GluN2B subunit-containing NMDA receptors in hippocampal plasticity. *Philos. Trans. R. Soc. Lond. B Biol. Sci.* **369**, 20130163.

Sultana R., Banks W. A. and Butterfield D. A. (2010) Decreased levels of PSD95 and two associated proteins and increased levels of BCl2 and caspase 3 in hippocampus from subjects with amnestic mild cognitive impairment: insights into their potential roles for loss of synapses and memory, accumulation of Abeta, and neurodegeneration in a prodromal stage of Alzheimer's disease. *J. Neurosci. Res.* **88**, 469–477.

Togashi H., Abe K., Mizoguchi A., Takaoka K., Chisaka O. and Takeichi M. (2002) Cadherin regulates dendritic spine morphogenesis. *Neuron* **35**, 77–89.

Trapp T., Olah L., Holker I., Besselmann M., Tiesler C., Maeda K. and Hossmann K. A. (2001) GTPase RhoB: an early predictor of neuronal death after transient focal ischemia in mice. *Mol. Cell Neurosci.* **17**, 883–894.

Troyanovsky S. (2005) Cadherin dimers in cell-cell adhesion. *Eur. J. Cell Biol.* **84**, 225–233.

Urabe M., Ding C. and Kotin R. M. (2002) Insect cells as a factory to produce adeno-associated virus type 2 vectors. *Hum. Gene Ther.* **13**, 1935–1943.

Utreras E., Maccioni R. and González-Billault C. (2009) Cyclin-dependent kinase 5 activator p35 over-expression and amyloid beta synergism increase apoptosis in cultured neuronal cells. *Neuroscience* **161**, 978–987.

Wildenberg G. A., Dohn M. R., Carnahan R. H., Davis M. A., Lobdell N. A., Settleman J. and Reynolds A. B. (2006) p120-catenin and p190RhoGAP regulate cell-cell adhesion by coordinating antagonism between Rac and Rho. *Cell* **127**, 1027–1039.

Zhang S., Edelmann L., Liu J., Crandall J. E. and Morabito M. A. (2008) Cdk5 regulates the phosphorylation of tyrosine 1472 NR2B and the surface expression of NMDA receptors. *J. Neurosci.* **28**, 415–424.